

A WAVE THEORETIC METHOD FOR ESTIMATING THE EFFECTS OF
INTERNAL TIDES UPON ACOUSTIC WAVE TRANSMISSION

D. J. Ramsdale

Naval Research Laboratory, Washington, DC 20375
U.S.A.

ABSTRACT

The effect of the first mode semidiurnal internal tide on a duct-type sound speed profile was approximated by varying the minimum velocity of the parabolic profile in a sinusoidal fashion with a period of 12.42 hours. The corresponding effect on the acoustic field was determined by using the normal mode solutions to the parabolic profile to compute the signal level and phase at a fixed receiver due to a fixed cw source. A systematic computer study was performed to determine the dependence of signal level and phase upon the source frequency, receiver range and tidal amplitudes. Numerical results showed that the acoustic phase variation over a tidal cycle was very nearly a sinusoid with 12.42 hour period and a peak-to-peak amplitude which was approximately a linearly increasing function of source frequency, receiver range and tidal amplitude. A simple analytical expression was developed which predicts these linear dependencies and closely approximates the phase variations computed numerically. The fluctuations in signal level during a tidal cycle were found to depend upon the detailed structure of the acoustic field in the immediate vicinity of the receiver. In general, however, the fluctuations in signal level increased in frequency with increasing source frequency, tidal amplitude and receiver range.

I. INTRODUCTION

Large-scale periodic motions exist in the ocean in the form of internal waves. The effect of these motions upon the passage of an acoustic wave through the ocean has received a great deal of attention in the recent literature.¹⁻¹⁸

Of particular relevance to the results presented in this paper are the experimental work of Clark and Kronengold¹⁴ and the associated theoretical analyses of Weinberg, Clark and Flanagan.¹² The experiment conducted by Clark and Kronengold involved transmitting a 406 Hz cw signal from Eleuthera, Bahamas, to hydrophones in the Eleuthera-Bermuda Propagation Range. Signals received at both Bermuda and intermediate hydrophones approximately 500 km from the source showed that the extended angle phase variation was dominated by a large semidiurnal component, suggesting that the acoustic propagation in that region was strongly influenced by a deep ocean internal tide of characteristic M2 periodicity, 12.42 hours.

The terminology "extended angle phase" means that the phase variation through more than one complete cycle is recorded as such, rather than as an angle between 0° and 360°. The distortion of the sound speed profile due to the motion of the first mode semidiurnal internal tide has been determined by Mooers.¹⁸ For the case in which the acoustic path is perpendicular to the direction of propagation of the internal tide, Weinberg, Clark

and Flanagan varied the sound speed profile according to Mooer's prescription, using a ray-trace model to compute the associated time history of transmission loss and phase of the acoustic signal during a 12.42 hour tidal cycle. Their calculations for 406 Hz and a range of approximately 500 km showed that (1) the peak-to-peak variation in extended angle phase was linearly proportional to the amplitude of the internal tide and (2) the fluctuation in transmission loss became greater in extent and more rapid with increasing tidal amplitude.

In this paper, we report the results of a normal mode calculation using the parabolic profile in which the profile is varied to crudely approximate the effect of the first mode semidiurnal internal tide. The extended angle phase and signal level are computed as functions of source frequency, receiver range and internal tidal amplitude. Approximate analytical expressions are developed to predict the dependence of extended angle phase on these parameters and an explanation is offered for the computed fluctuations in signal level.

II. THE MODEL

The parabolic profile is one of the few for which exact closed-form solutions are available.¹⁹⁻²² The acoustic pressure (p) at a range (r) and depth (z) due to a point source of angular frequency (ω) placed at the origin in range and depth z_0 is given by

$$p = \frac{\omega \rho}{4} \sum_{n=0}^{\infty} \left(\frac{2}{\pi k_n r} \right)^{1/2} \exp i \left(k_n r - \pi/4 - \omega t \right) \times \exp \left[\frac{-\beta^2}{2} \left(z^2 + z_0^2 \right) \right] \frac{H_n(\beta z) H_n(\beta z_0)}{2^n n! \sqrt{K\alpha/\pi}} \quad (1)$$

where ρ is the density, H_n are the hermite polynomials of order n , $K = \omega/c_0$, $\beta^2 = K\alpha$ and the eigenvalues k_n are given by

$$k_n = [K^2 - (2n + 1) K\alpha]^{1/2} \quad (2)$$

For any set of source/receiver parameters the pressure can be written as

$$p = A \exp i(\phi - \omega t) \quad (3)$$

where the pressure amplitude A and phase ϕ are determined from the real and imaginary parts of Eq. (1) (suppressing the harmonic time dependence).

The solutions to the truncated parabolic profile, shown in Fig. 1, are very nearly those for the parabolic profile in which modes with phase velocities greater than c_1 , the velocity at the edge of the duct are ignored.²² In all our calculations the infinite sum in Eq. (1) is replaced by a finite sum in which $c_n = \omega/k_n < c_1$. This represents a more realistic model for fluctuations since it restricts the range of values of k_n to those normally encountered in the real ocean.

The distortion of the sound speed profile predicted by Mooers¹⁸ as due to the first mode semidiurnal internal tide is shown in Figure 2. This rhythmic movement in the profile can be approximated crudely using the parabolic profile by varying the axial sound speed c_0 according to

$$c_0 = \bar{c}_0 + \Delta c_0 \sin \Omega t \quad (4)$$

where Ω is the tidal frequency and \bar{c}_0 is the unperturbed speed at the axis. The sound speed perturbation produced by the action of the internal wave has been shown to be very nearly proportional to the internal wave amplitude.¹⁸ Thus, the value of Δc_0 in Eq. (4) can be regarded as proportional to the internal wave amplitude.

Given the source location, frequency transmitted and receiver location, a time history of the amplitude and extended angle phase can be generated using the parabolic profile (terminated as in Figure 1) with the axial velocity c_0 given in Eq. (4). In performing the computation, the extended angle phase was determined by increasing or decreasing the phase by one cycle as appropriate when the phase angle moved from quadrants one to four or vice versa; the time sampling interval was chosen sufficiently small to facilitate the phase tracking. The amplitude was represented in dB by taking $20 \log A$ and plotted in dB as a loss in signal level.

III. NUMERICAL RESULTS

All calculations were made with both source and receiver on the axis of the parabola, the unperturbed profile specified by $c_0 = 1480$ m/sec, $c_1 = 1520$ m/sec and $h = 1000$ m. Typical results for a source frequency of 100 Hz, receiver range of 109.5 km (8th focal zone) and a $\Delta c = 1.0$ m/sec are shown in Figure 3. These are in general similar to those computed by Weinberg, et al.,¹² in that the extended angle phase is sinusoidal with a period identical to the tidal cycle, and the fluctuations in amplitude are of higher frequency, varying over some

15 dB. Note that the amplitude of the negative part of the extended angle phase is smaller by nearly one full cycle than that of the positive half. This is due to the two 180° phase changes encountered at each deep null in signal level during the negative portion of the cycle.

A. Dependence on tidal amplitude, source frequency and receiver range.

Dependence of the extended angle phase upon Δc_0 (tidal amplitude) was determined by simply holding frequency and range constant ($f = 100$ Hz, $r = 109.5$ km) and varying Δc_0 . The results are summarized in Figure 4, which shows that the peak-to-peak variation in extended angle phase is a linear function of Δc_0 , which is, of course, proportional to tidal amplitude. This result was also obtained by Weinberg, et al., using their ray-theory model which incorporated both the sea floor and surface and was thus considerably more complicated than the simple wave model used here.

Plots of the signal level as a function of time over a tidal cycle for these cases show that as the tidal amplitude increases, the peak-to-peak fluctuation in signal level increases while the time (τ) for the normalized autocorrelation of the signal level to drop to 0.5 decreases. The peak-to-peak fluctuation in signal level varies from 29.9 dB for $\Delta c_0 = 2.0$ to 2.1 dB for $\Delta c_0 = 0.25$ while the corresponding decorrelation times (τ) vary from 11.5 minutes to 55.5 minutes.

Dependence of the extended angle phase on source frequency was examined by holding the range and tidal amplitude constant

($r = 109.5$ km and $\Delta c_0 = 1.0$ m/sec) and varying the frequency. The results are summarized in Figure 5, which shows that the peak-to-peak variation in extended angle phase is a linear function of source frequency over the range 10 Hz to 400 Hz. Plots of signal level over the tidal cycle as a function of time showed that the peak-to-peak fluctuation increased while decorrelation time (τ) decreased with frequency, ranging from 29.9 dB and 8.25 minutes, respectively, at 400 Hz to 15.4 dB and 21 minutes, respectively, at 100 Hz, while for 10 Hz the corresponding values are 2.4 dB and a time greater than 70 minutes for 10 Hz.

Preliminary measurements have been made between a fixed source and a fixed receiver separated by some 400 nautical miles with source frequencies of 12 and 22 Hz.²³ Internal tides appeared to be modulating the phase, but the total phase change over a six-hour period was only a fraction of a cycle and the corresponding amplitude fluctuation approximately 1-2 dB. This gives credence to our theoretical results which showed that both phase and amplitude fluctuations decrease with decreasing source frequency.

The dependence of extended angle phase on receiver range was determined by keeping the source frequency and tidal amplitude constant ($f = 100$ Hz and $\Delta c_0 = 1.0$ m/sec) and varying the receiver range. The results of such calculations carried out over ranges from 100 to 420 km are shown in Figure 6. The dependence is approximately linear but deviations are more

noticeable than in the case of frequency or tidal amplitude. These deviations are a result of phase changes due to deep fades in the signal level; thus, even though the value taken from the linear curve would be a good estimate of the peak-to-peak variation in extended angle phase at a given range, deviations can result if the amplitude structure displays deep nulls.

The complexity and variation in signal level at each of the various ranges depends on whether one is near a focal zone or between a focal zone. For example, at a range of 109.5 km (8th focal zone) the peak-to-peak fluctuation in signal level is 15.4 dB with a decorrelation time of 21 minutes, while at 117 km (between 8th and 9th focal zones) the corresponding numbers are 2.8 dB and 13.5 minutes. In general, the variations in signal level and decorrelation times are larger near focal zones than in between them. Also, in general, for both zones, focal and non-focal, the variations in signal level increase while the decorrelation times decrease as range increases.

B. Random component of axial velocity

The speed of sound near the sound channel axis is surprisingly variable.²⁴ To investigate the effect of a small random variability on the signal level and extended angle phase, a small amount of speed randomly selected in time from a normal distribution was added to the axial velocity in addition to that due to the internal tide. The magnitude of the random

component was determined by specifying the standard deviation of a normal distribution whose mean value was zero. The signal level, its autocorrelation function and the extended angle phase were computed over a tidal cycle for a constant range ($r = 109.5$ km) and constant tidal amplitude ($\Delta c_0 = 1.0$ m/sec) for frequencies of 10 Hz, 100 Hz, 200 Hz and 400 Hz with the addition of a random axial velocity component determined by a standard deviation of 0.01 m/sec. These results were compared with identical calculations where the random axial component was zero. The effect of the random component upon the 10 Hz and 100 Hz results was negligible. The peak-to-peak extended angle phase at 200 Hz was 14.35 cycles with the random component as compared to 17.06 cycles without it; however, the basic sinusoid shape, although contaminated by a certain amount of "grass," was still retained. The results for the 400 Hz source are shown in Figure 7. In this case, the random component was large enough to prohibit phase tracking. Although a certain amount of "grass" was added to the signal level curves at all frequencies, the decorrelation time was substantially the same both with and without the random component.

An additional set of computations were performed with all parameters as before but with the standard deviation of the random component now set at 0.1 m/sec. The extended angle phase for the 10 Hz source was quite grassy but still basically sinusoid, and the decorrelation time was still greater than 70 minutes as in the case of no random component. However, for the 100 Hz,

200 Hz and 400 Hz cases the sinusoidal phase variation was destroyed and the signal level decorrelated in approximately one minute.

These results show that a random component in the axial velocity discriminates more against tracking phase variations due to internal tides at high acoustic frequencies than at low acoustic frequencies. This suggests that perhaps the effects of an internal tide might be masked at a high acoustic frequency while being visible at a lower acoustic frequency. The decorrelation time is not as sensitive as phase to random components in the axial velocity but eventually will be increased as the standard deviation of the random component increases.

IV. ANALYSIS

Numerical results presented in the previous section showed that the peak-to-peak value of extended angle phase is to a good approximation linearly dependent upon receiver range, source frequency and tidal amplitude. Calculations of extended angle phase as a function of range for source and receiver on the axis with a source frequency of 100 Hz showed that with the exception of deep nulls in amplitude, the phase can be represented fairly well by $\phi = kr$. The exact value one uses for k depends upon the modes which contribute most to the solution and their speeds but consider for the moment that $k = \omega/c$ where c represents some typical sound speed. The internal tide causes a variation in c with time so that the resulting phase variation

can be written as

$$\Delta\phi(r,t) = -\left(\frac{1}{c^2}\right) \omega r \Delta c \sin \Omega t \quad (5)$$

which demonstrates very simply the numerically observed linear dependence on tidal amplitude (Δc), source frequency, and range. Note that it correctly predicts a phase variation which is 180 degrees out of phase with the driving function.

The prediction of accurate values of extended angle phase using Eq. (5) depends to some extent on the particular choice of c and Δc . Consider the case computed numerically in the previous section of a source/receiver on the axis, source frequency 100 Hz, $\Delta c=1$ m/sec and receiver range of 109.5 km. Taking c to be 1500 m/sec one finds a peak-to-peak value of 9.73 cycles which is in reasonable agreement with the true value of 8.65 as determined numerically. Suppose we consider applying Eq. (5) to the case computed by Weinberg, et al., where a 406 Hz source was located approximately 500 m from the surface propagating acoustic energy to a receiver some 500 km away at a depth greater than 2000 m while the medium was under the influence of a 10-m internal tide. If we take as c the sound speed at the SOFAR axis and Δc the maximum change in the axis speed produced by the internal wave, Eq. (5) predicts a peak-to-peak phase variation of 27.4 cycles, which compares perhaps fortuitously to the value of 25 cycles computed by Weinberg, et al.¹² This suggests that perhaps a rule of thumb in using Eq. (5) is to take c equal to the speed at the SOFAR axis and Δc as the maximum change in this speed.

Now let us consider the fluctuations in signal level. In an effort to understand these fluctuations, several computations were made of the signal level as a function of range for slightly different values of c_0 . The results showed that the acoustic field for two values of c_0 very nearly the same was the same in form but shifted slightly in range. The amount of range shift can be approximated well by computing the change in spacing (R) between focal zones as c_0 changes. Since $R = \pi/\alpha$ (source and receiver on the axis),

$$\Delta R = \frac{R c_0 \Delta c_0}{c_1^2 - c_0^2} \quad (6)$$

Application of this expression to the case where the receiver is at the 8th focal zone ($r = 109.5$ km) yields a shift in range of approximately 1.3 km. Figure 8 shows the corresponding signal level as a function of range for a source frequency of 100 Hz, the dotted lines indicating the range shift corresponding to $\Delta c_0 = 1.0$ m/sec centered at 109.5 km. Note that the portion of the signal within the dotted lines when sampled in a sinusoidal manner beginning at 109.5 km corresponds to the fluctuations in signal level shown in Figure 3.

A close study of the plots of transmission loss over a tidal cycle for various tidal amplitudes as computed by Weinberg, et al. (reproduced in Figure 9) leads one to the same conclusion, i.e., the effect of the internal tide is mainly to move the acoustic field back and forth in range. This can be seen in

Figure 9 by noting that a larger tidal amplitude causes the field to shift greater in range; thus, the fluctuations for a 7-m internal tide would be included as a subset of those for a 10-m internal tide. Examination of Figure 9 shows this to be the case.

According to Eq. (6), the amount of range shift depends directly upon the tidal amplitude (Δc_0) and the range (number of focal zones covered), but is independent of frequency. One conclusion reached then is that the fluctuations in signal level at any range depend upon the structure of the acoustic field nearby, since the effect of the internal tide is simply to sample the field nearby the range in question. Thus, if the acoustic field has a great deal of structure due to interference effects, the fluctuations in signal level due to the internal tide will increase in frequency and perhaps magnitude with tidal amplitude and/or range. The dependence of the signal level fluctuations on frequency is due simply to the higher frequencies having more modes contributing to the results which in turn produces a more complex interference structure in the acoustic field.

V. SUMMARY

The effect of the first mode semidiurnal internal tide upon acoustic wave propagation has been estimated using the normal mode solutions to the parabolic velocity profile. The action of the internal tide on the parabolic velocity profile was approximated by allowing the minimum velocity to vary

in a sinusoidal fashion, having a 12.42 period with the maximum variance from the unperturbed value taken to be proportional to the internal tidal amplitude. A systematic computer study was performed to determine the dependence of signal level and extended angle phase on the source frequency, receiver range and tidal amplitude. The results showed that the extended angle phase was very nearly a linear function of all three parameters. No such simple result was obtained for fluctuations in signal level, although in general the extent and frequency of these fluctuations increased with higher source frequency, greater tidal amplitude and greater receiver range.

Further computer studies using an unperturbed parabolic profile showed that as range increased, the phase was fairly well approximated by the product of wavenumber and range. This fact lead to the development of a simple formula which predicts linear dependence of extended angle phase on source frequency, receiver range and tidal amplitude. Values of extended angle phase computed using this simple expression are in reasonable agreement with those obtained numerically and also with those computed by Weinberg, et al.¹²

Fluctuations in signal were traced to the fact that the effect of the internal tide was to shift the acoustic field in range, the amount increasing linearly with range and tidal amplitude. Again, a simple analytic expression was determined which approximates this shift. The fluctuations in signal level at any range then depend upon the structure of the acoustic field nearby, but generally will increase in frequency with increasing tidal amplitude and range. The effect of source

frequency upon signal level fluctuations is mainly through the increasing complexity of the field with increasing source frequency; thus, for a constant range and tidal amplitude, signal level fluctuations decorrelate faster as frequency increases.

References

1. S. D. Chuprov, "On the Observation of a Sound Signal in the Presence of Internal Waves," *Izv. Atmos. and Oceanic Phys.* 2, 551-552 (1966).
2. E. J. Katz, "Effect of the propagation of internal water waves on underwater sound transmission," *J. Acoust. Soc. Am.* 42, 83-87 (1967).
3. J. C. Beckerle, J. L. Wagar and R. D. Worley, "Underwater Acoustic Wavefront Variations and Internal Waves," *J. Acoust. Soc. Am.* 44, 295-296 (1968).
4. J. C. Steinberg, J. G. Clark, H. A. DeFerrari, M. Kronengold and K. Yacoub, "Fixed System Studies of Underwater Acoustic Propagation," *J. Acoust. Soc. Am.* 52, 1521-1536 (1972).
5. R. N. Baer and M. J. Jacobson, "Sound Transmission in a Channel with Bilinear Sound Speed and Environmental Variations," *J. Acoust. Soc. Am.* 54, 80-91 (1973).
6. Weston, D. E. and H. W. Andrews, "Acoustic Fluctuations due to Shallow Water Internal Waves," *J. Snd. and Vib.* 31, 357-368 (1973).
7. R. N. Baer and M. J. Jacobson, "Analysis of the Effect of a Rossby Wave on Sound Speed in the Ocean," *J. Acoust. Soc. Am.* 55, 1178-1189 (1974).
8. H. A. DeFerrari, "Effects of Horizontally Varying Internal Wavefields on Multipath Interference for Propagation through the Deep Sound Channel," *J. Acoust. Soc. Am.* 56, 40-46 (1974).
9. R. H. Clarke, "Sound Propagation in a Variable Ocean," *J. Sound and Vib.* 34, 457-477 (1974).
10. *Ibid.*, "Transmission of Underwater Sound through Internal Waves and Turbulence," *Proceedings of the Satellite Symposium on Underwater Acoustics*, 8th ICA, August, 1974.
11. R. C. Spindel, R. P. Porter and R. J. Jaffee, "Long-Range Sound Fluctuations with Drifting Hydrophones," *J. Acoust. Soc. Am.* 56, 440-446 (1974).
12. N. L. Weinberg, J. G. Clark and R. P. Flanagan, "Internal Tidal Influence on Deep-Ocean Acoustic-ray Propagation," *J. Acoust. Soc. Am.* 56, 447-458 (1974).
13. R. N. Baer and M. J. Jacobson, "Effect of a Rossby Wave on the Phase of an Underwater Acoustic Signal," *J. Acoust. Soc. Am.* 56, 809-816 (1974).

14. J. G. Clark and M. Kronengold, "Long-period Fluctuations of cw signals in Deep and Shallow Water," *J. Acoust. Soc. Am.* 56, 1071-1083 (1974).
15. R. C. Spindel, R. P. Porter and R. J. Jaffee, "Acoustic-internal Wave Interaction at Long Ranges in the Ocean," *J. Acoust. Soc. Am.* 56, 1426-1436 (1974).
16. V. A. Polyanskaya, "Influence of high-frequency internal waves on the sound field of a point source in the ocean," *Sov. Phys. Acoust.* 20, 55-59 (1974).
17. R. N. Baer and M. J. Jacobson, "SOFAR transmission fluctuations produced by a Rossby Wave," *J. Acoust. Soc. Am.* 57, 569-576 (1975).
18. C. N. K. Mooers, "Sound-velocity Perturbations Due to Low-frequency Motions in the Ocean," *J. Acoust. Soc. Am.* 57, 1067-1075 (1975).
19. H. Uberall and N. C. Nicholas, "Range Focusing in a Deep-Ocean Sound Channel with Parabolic Profile," *J. Acoust. Soc. Am.* 44, 1259-1261 (1968).
20. N. C. Nicholas and H. Uberall, "Normal-Mode Propagation Calculations for a Parabolic Velocity Profile," *J. Acoust. Soc. Am.* 48, 745-752 (1970).
21. N. C. Nicholas, "The Propagation of Sound in the Deep Ocean: A Wave Formulation," AD-754-371, pp. 131, September, 1971.
22. I. Tolstoy and C. S. Clay, *Ocean Acoustics*, McGraw-Hill, New York, 1966, pp. 87-93 and pp. 178-180.
23. K. D. Flowers, Naval Research Laboratory, private communication.
24. Ants T. Piip, "Fine Structure and Stability of the Sound Channel in the Ocean," *J. Acoust. Soc. Am.* 36, 1948-1953 (1964).

FIG. 1
TRUNCATED PARABOLIC PROFILE.
 $c(z) = c_0 [1 - \alpha^2 z^2]^{-\frac{1}{2}}$ WHERE
 $\alpha = \frac{1}{h} \left[1 - \left(\frac{c_0}{c_1} \right)^2 \right]^{\frac{1}{2}}$
 AND $|z| < h$

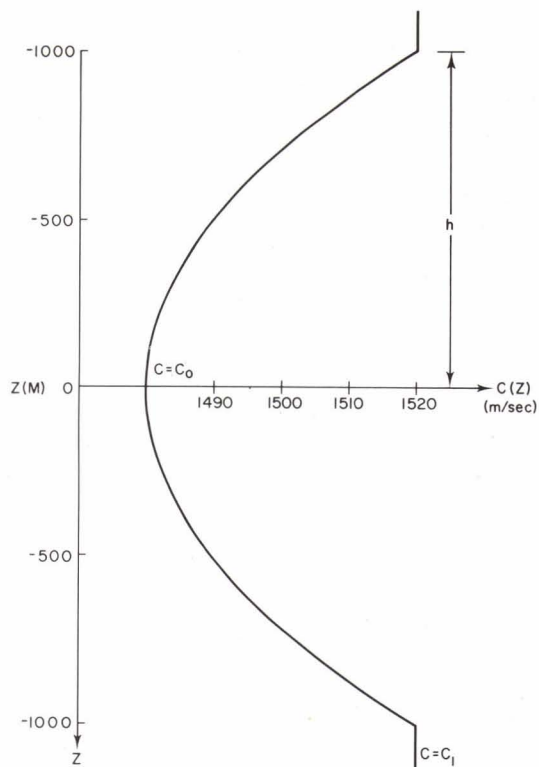


FIG. 2
MEAN SOUND SPEED AND PERTURBATION ENVELOPE
 [From Mooers, 18]

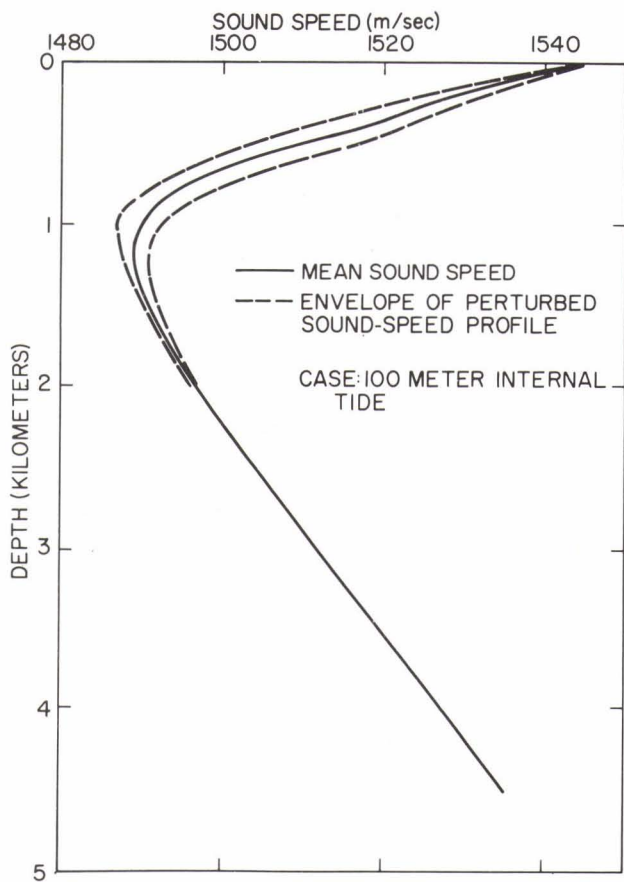
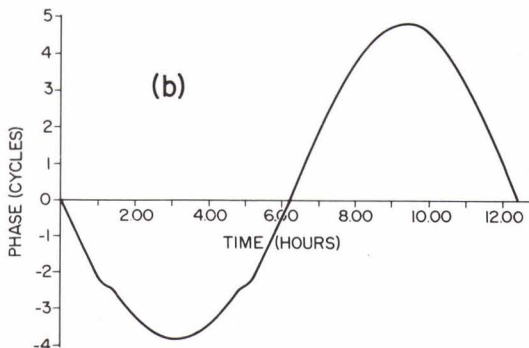
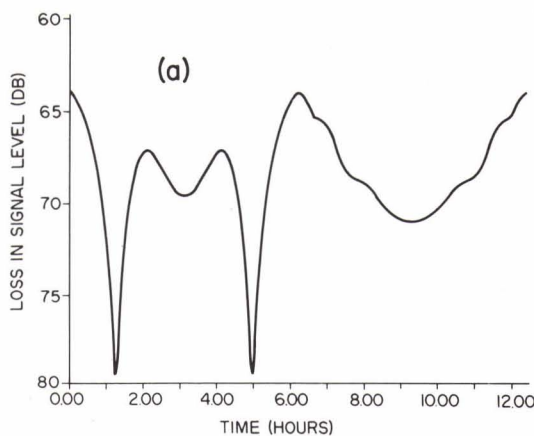


FIG. 3
ACOUSTIC TIME SERIES FOR A SOURCE FREQUENCY
OF 100 Hz, A RECEIVER RANGE OF 109.5 km (8th
FOCAL ZONE) AND A $\Delta c_0 = 1.0$ m/sec



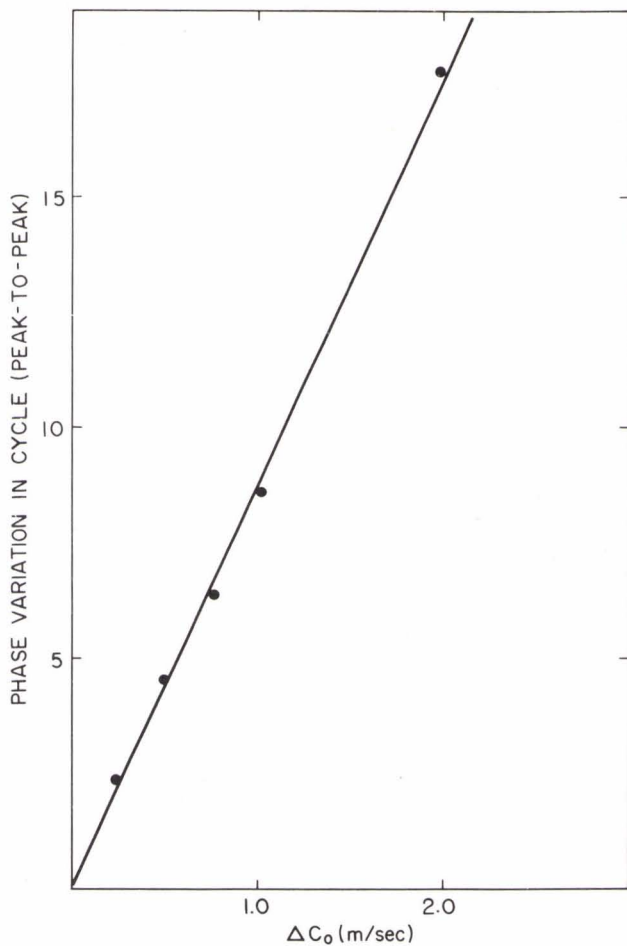
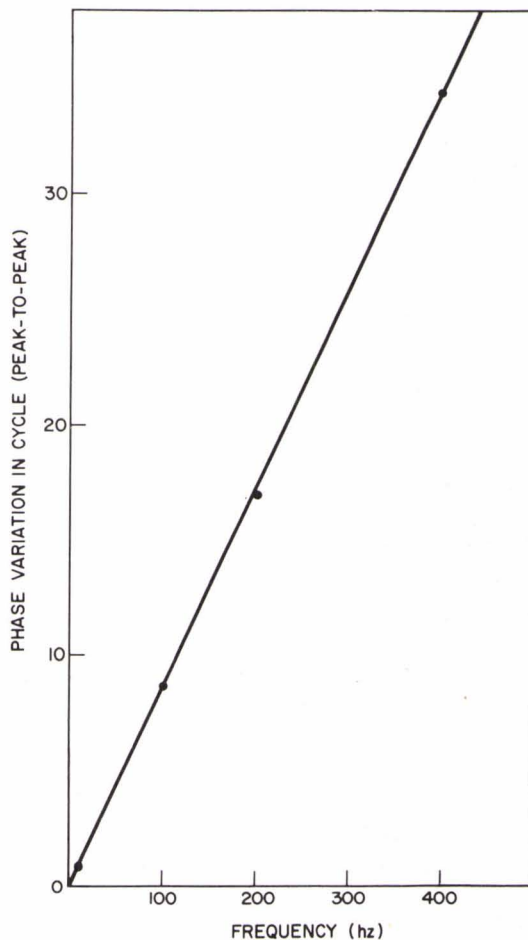


FIG. 4
PHASE VARIATIONS AS A FUNCTION OF TIDAL AMPLITUDE ($\sim \Delta c_0$) FOR A SOURCE FREQUENCY OF 100 Hz AND A RECEIVER RANGE OF 109.5 km

FIG. 5
PHASE VARIATIONS AS A FUNCTION OF FREQUENCY FOR A RECEIVER AT 109.5 km WITH A CONSTANT TIDAL AMPLITUDE ($\Delta c_0 = 1.0$ m/sec)



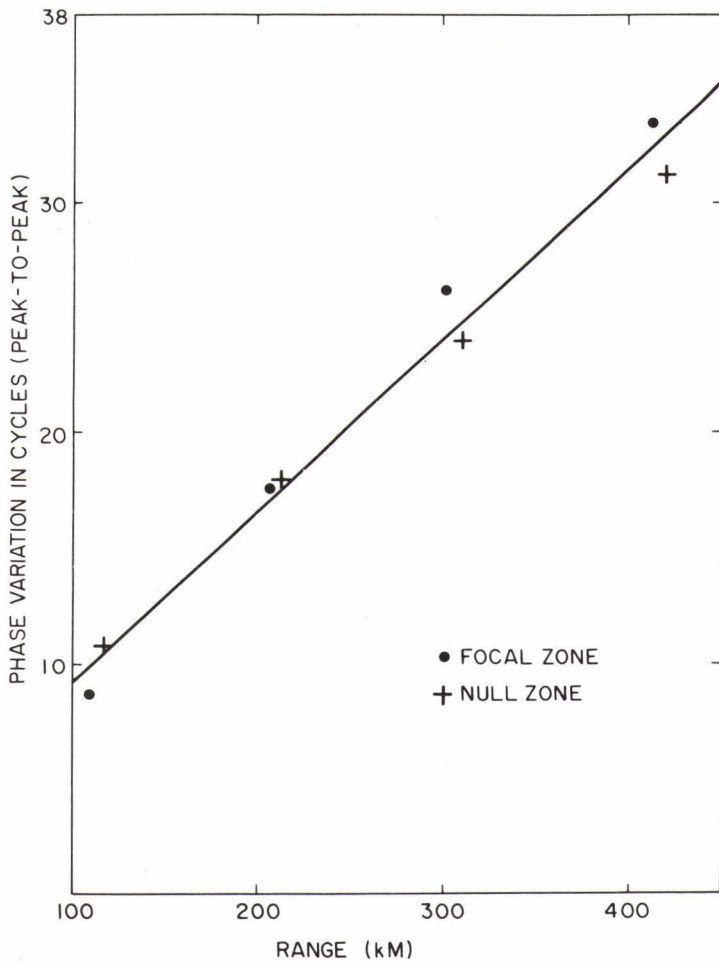
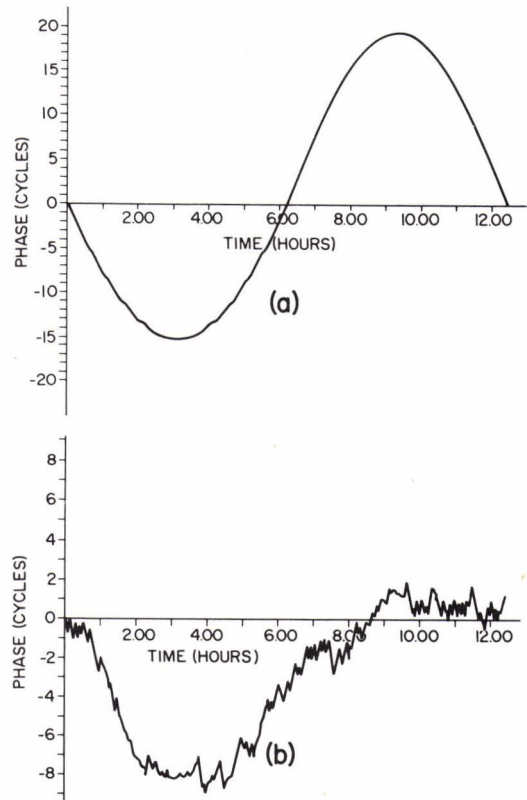


FIG. 6
PHASE VARIATIONS AS A FUNCTION OF RANGE FOR
A CONSTANT SOURCE FREQUENCY (100 Hz) AND
CONSTANT TIDAL AMPLITUDE ($\Delta c_o = 1.0$ m/sec)

FIG. 7
EXTENDED ANGLE PHASE FOR A SOURCE FREQUENCY
OF 400 Hz, RECEIVER RANGE OF 109.5 km, $\Delta c_o = 1.0$
m/sec WITH (a) NO RANDOM COMPONENT IN THE
AXIAL VELOCITY AND (b) A GAUSSIAN-DISTRIBUTED
RANDOM COMPONENT WITH STANDARD DEVIATION OF
1 cm/sec ADDED TO THE AXIAL VELOCITY



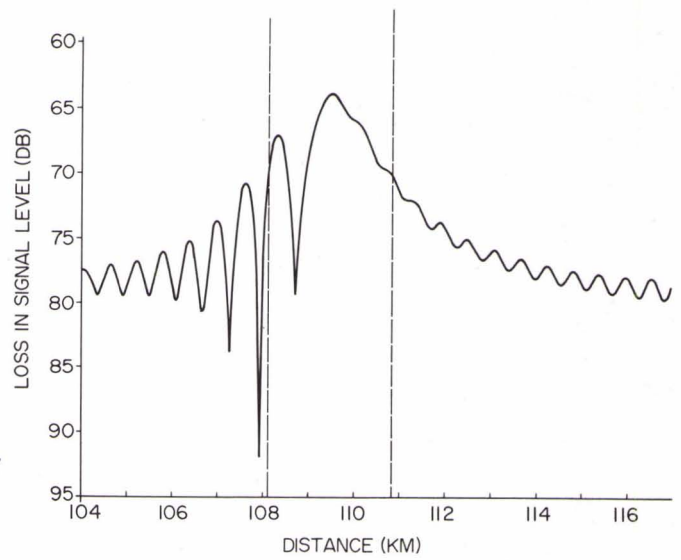


FIG. 8
SOURCE/RECEIVER ON THE AXIS, SOURCE FREQUENCY
100 Hz

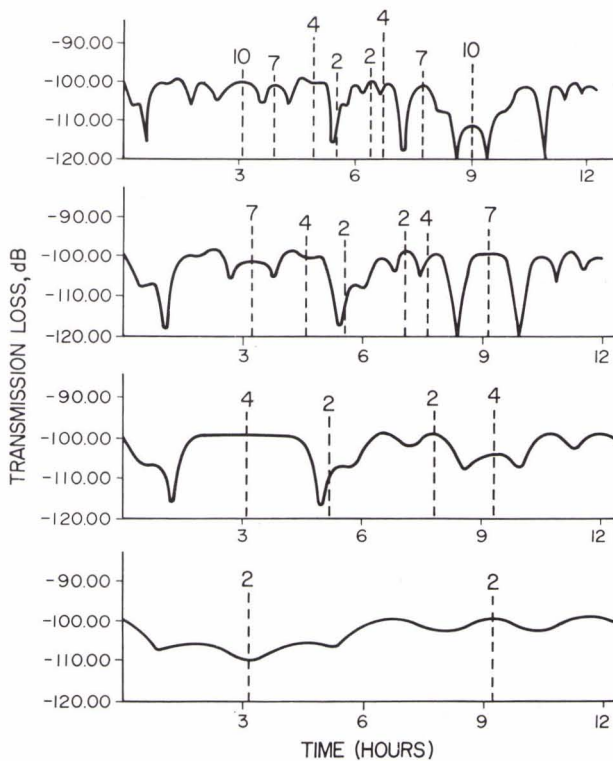


FIG. 9
TRANSMISSION LOSS OVER A TIDAL CYCLE FOR TIDAL
AMPLITUDES OF 10, 7, 4 AND 2 m, TOP TO BOTTOM